JCTC Journal of Chemical Theory and Computation

Article

pubs.acs.org/JCTC

Unraveling Interactions in Molecular Crystals Using Dispersion Corrected Density Functional Theory: The Case of the Epoxydihydroarsanthrene Molecules

A. Otero-de-la-Roza,*[,†] Víctor Luaña,*[,‡] Edward R. T. Tiekink,*[,¶] and Julio Zukerman-Schpector*[,§]

[†]National Institute for Nanotechnology, National Research Council of Canada, 11421 Saskatchewan Drive, Edmonton, Alberta, Canada T6G 2M9

[‡]Departamento de Química Física y Analítica, Facultad de Química, Universidad de Oviedo, 33006 Oviedo, Asturias, Spain

[¶]Department of Chemistry, University of Malaya, 50603 Kuala Lumpur, Malaysia

[§]Laboratório de Cristalografía Estereodinâmica e Modelagem Molecular, Departamento de Química, Universidade Federal de São Carlos, São Carlos, SP 13565−905, Brazil

ABSTRACT: Noncovalent interactions are prevalent in crystal packing and supramolecular chemistry. Directional noncovalent interactions such as donor−acceptor bonds (e.g., hydrogen, chalcogen, and pnictogen bonds) as well as nondirectional forces (such as dispersion) come together to stabilize supramolecular assemblies by striking a delicate energetic balance. Typically, a two-pronged approach employing experimental X-ray structures and gas phase quantum chemical modeling has been used to understand and design supramolecular architectures. Drawing from recent advances in molecular crystal modeling with dispersion corrected density functional theory (DFT), we propose in this article a combination of qualitative noncovalent index (NCI) analysis and periodic and gas phase DFT calculations on substitutional crystal analogues to unravel the dominant interactions in a particular crystal packing. We illustrate the possibilities of this approach by studying three crystal packings of epoxydihydroarsanthrene analogues that present a complex combination of donor−acceptor interactions including pnictogen-pnictogen, pnictogen-π, and pnictogen-chalcogen. We show that, in these crystals, the chalcogen-pnictogen interaction dominates over the pnictogen-pnictogen and pnictogen-π. In the latter, the role of donor and acceptor is reversed depending on the interacting moieties. Multiple chalcogen-pnictogen interactions necessitate larger donor atoms, such as sulfur. These observations explain and rationalize the experimentally observed crystal structures.

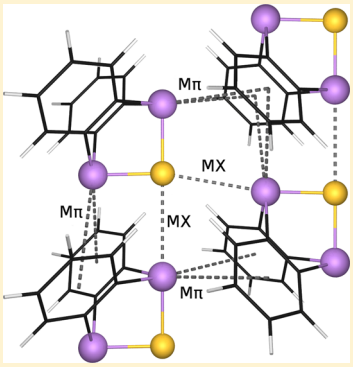

1. INTRODUCTION

The fundamental objective in crystal engineering[1−5] is to explain and ultimately predict crystal structures based on known intra- and intermolecular interactions. Success in both endeavors hinges on an accurate appraisal of the forces that determine the structure of a crystal packing or a supramolecular aggregate. Consequently, there is an ongoing interest[6] in the development of methods to probe the leading contributions that determine the stability of a given supramolecular architecture.

To study intermolecular interactions, crystal engineers have two primary tools at their disposal: statistical analysis of databases[6−10] and quantum mechanical studies of intermolecular motif models.[11−14] Database analyses use distance and angle criteria to determine if two moieties are interacting. Quantum chemical modeling involves the calculation of dimer binding energies in the gas phase and perhaps their components in some energy partitioning scheme. The chosen dimers resemble the bonding patterns, but they are idealized so as to isolate a particular interaction. A common procedure is to study substitutional analogues of the same dimer: by replacing certain atoms (N by P, for instance) or moieties (e.g., benzene by hexafluorobenzene) it is possible to gain information about the behavior of the interaction in different chemical environments.[13]

A menagerie of synthons has been identified and studied using these approaches,[8,9,11,13,15−17] but their importance in observed crystal structures often does not correlate with their gas phase binding energies.[6] Ultimately, the assignment of the dominant patterns from X-ray data in a particular crystal is subjective[1] because there is no way to quantify from the structure alone how much a certain motif contributes to the lattice energy, which is a problem in crystals presenting more than one "obvious" pattern.[6] Even in crystals where there is a clear dominant interaction, said interaction only accounts for only a fraction of the total lattice energy.[6,18]

Dispersion corrected density functional theory (dcDFT) has experienced tremendous advances in the past few years.[19,20] Nowadays it is possible to calculate lattice energies of molecular crystals to an accuracy of ∼1 kcal/mol[18] and lattice energy differences with a much reduced error.[21] The success in recent

Received: September 12, 2014
Published: October 9, 2014

   dx.doi.org/10.1021/ct500832g | J. Chem. Theory Comput. 2014, 10, 5010−5019

blind crystal structure prediction tests is a testimony of the progress in the field.[22,23] In this article, we use periodic dcDFT to study and quantify the importance of different intermolecular interactions in crystal packing.

In this approach, for a given molecular crystal structure (obtained from experimental diffraction data), we replace certain atoms with analogous elements in order to introduce steric and electronic effects without grossly modifying the molecular or the crystal structure. The geometry of the resulting crystals is relaxed, and information is extracted from the lattice energy and the interatomic distances. This approach is equivalent to the traditional model dimer studies but in the context of the actual crystal packing. The equilibrium crystal structures represent the optimal (minimum energy) packing of the molecules in that particular arrangement. The resulting electron densities can be used to identify the relevant intermolecular interactions with the noncovalent interaction index (NCI) technique.[24,25] In addition, we calculate gas phase binding energies for the relevant interacting dimers in order to determine the leading contribution to the lattice energy and the relative importance of each interaction.

As a proof of concept example, we study the crystal structure of 5,10-epoxy-5,10-dihydroarsanthrene, whose structure is shown in Figure 1, and two of its derivatives: the same

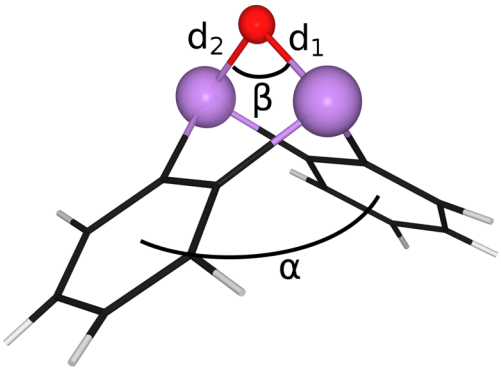

Figure 1. 5,10-Epoxy-5,10-dihydroarsanthrene molecule ($As_2(C_6H_4)_2O$) is the EPXARS crystal monomer. FEPXAS comprises the same molecule with all H replaced by F. EPSARS is formed by the EPXARS monomer with S instead of O. The atoms are As (purple large ball), O (red small ball), C (black sticks), and H (silver sticks). The labeled distances and angles will be used later in the article.

molecule with perfluorinated phenyl rings and the derivative where O is replaced by S. These crystal structures (shown in Figure 2) are particularly interesting because there is a mixture of donor−acceptor interactions (As···As, As···π, As···O). Original interest in these structures arose during an evaluation of putative As···π interactions in molecular crystal structures.[8] The structure of the epoxydihydroarsanthrene crystal presented two such interactions, and the nature of these was unclear, which prompted a theoretical investigation.

In this work, we show that, in these crystals, pnictogen-chalcogen is the dominant contribution and that the experimentally observed crystal structures can be explained by (i) the weakening of the As···π and As···O interactions upon fluorination and (ii) the ability of the larger sulfur atom to engage as donor in more than one donor−acceptor intermolecular bond. We also show that the substitutional analogues may form structures where the distinction between intermolecular and intramolecular bonds is blurred owing to

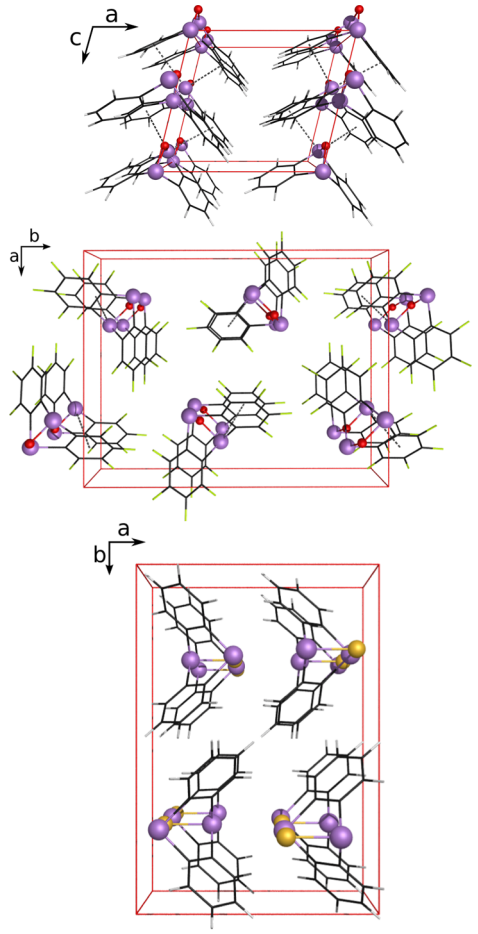

Figure 2. EPXARS (top), FEPXAS (middle), and EPSARS (bottom) crystal structures. The atom types are the same as in Figure 1.

extreme donor−acceptor interaction and that packing stabilization coming from dispersion is more important than suggested by the gas phase dimer results, with a contribution in excess of the total lattice energy.

2. CRYSTAL STRUCTURES

In this work, we study the intermolecular interactions in the crystal structures shown in Figure 2. The structure of the constituent monomers is shown in Figure 1. These molecules are composed of two pnictogen and one chalcogen atom and two π rings. In particular, the crystals shown in the figures correspond to the 5,10-epoxy-5,10-dihydroarsanthrene ($As_2(C_6H_4)_2O$) molecule, its perfluorinated version ($As_2(C_6F_4)_2O$), and 5,10-epithio-5,10-dihydroarsanthrene ($As_2(C_6H_4)_2S$). We will refer to them in the rest of the article as EPXARS,[26] FEPXAS,[27] and EPSARS,[28] respectively, after their Cambridge Structural Database (CSD) refcodes.[7] EPXARS forms two-dimensional layers, FEPXAS forms one-dimensional chains where the monomers stack on top of each other, and EPSARS forms parallel stacks of molecules with almost orthogonal S−As···S−As··· linear motifs in the ab plane (see Figure 3).

Due to the amphoteric character of the heavy pnictogens present in these molecules,[3] FEPXAS and particularly EPXARS and EPSARS present multiple directed bonding interactions including pnictogen-pnictogen, pnictogen-π, chalcogen-pnictogen, and chalcogen-halogen. These interactions belong to the

dx.doi.org/10.1021/ct500832g | J. Chem. Theory Comput. 2014, 10, 5010−5019

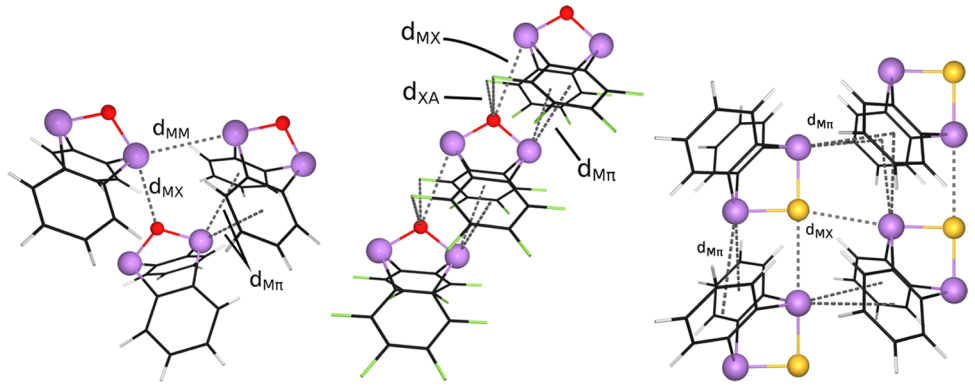

Figure 3. Motifs in the EPXARS (left), FEPXAS (middle), and EPSARS (right) crystals are shown. The atom types are the same as in Figure 1, and the yellow spheres refer to sulfur.

class of donor−acceptor noncovalent interactions, in which an electron donor (be it a π system, a chalcogen, a pnictogen, or any other electron rich source) interacts with the antibonding orbital (σ-hole) of the acceptor molecule. This class encompasses chalcogen, halogen, and pnictogen bonding and partially hydrogen bonding as well.[13,14] Common features in this family are electron withdrawing substituents in the acceptor atom strengthen the interaction, the bonding usually induces a lengthening of the opposite σ bond in the acceptor, there is a marked directional character, and cooperative effects are important. Electron transfer in pnictogen bonds is known to be important,[13,16,29,30] and it is expected that a proper account of dispersion is necessary for the description of these interactions as well.[29,31]

Several questions arise from the examination of the crystal structures: which of the multiple interactions is dominant. Or, more precisely, can we quantify the importance of each donor−acceptor contact? Why does the hydrogenated monomer crystallize in EPXARS but the fluorinated molecule prefer FEPXAS? Why are there linear pnictogen-chalcogen motifs in EPSARS but not in EPXARS or FEPXAS? These are questions that are difficult (or impossible) to answer from the geometry alone and that we try to address in the rest of the article.

3. METHODS

We calculated the equilibrium geometries and lattice energies of the 24 crystals that result from replacing selected atoms in the EPXARS, FEPXAS, and EPSARS crystal structures, there being in effect three theoretical crystal structures (polymorphs) for each composition. Namely, we took all the combinations generated by the (As,Sb), (O,S), and (H,F) replacements. The (As,Sb) replacement affects the donor/acceptor character of the pnictogen, the (O,S) replacement modifies the chalcogen donor strength, and the (H,F) replacement changes the polarity of the π ring. In the following, we will use the label M for the pnictogen atom (As or Sb), X for the chalcogen (O or S), and A for the monovalent ring substituent (H or F).

The periodic calculations were carried out using density functional theory (DFT) in the plane waves/pseudopotentials approach using the Quantum ESPRESSO package.[32] Dispersion forces are important in the modeling of noncovalent interactions in general[20] and in the description of donor−acceptor interactions in particular,[17] and they are not correctly represented by common density functionals.[19,20] To address this problem, we use the exchange hole dipole moment (XDM) model of dispersion proposed by Becke and Johnson.[33−38] The XDM model permits the calculation of the environment dependent dispersion interaction coefficients to any order.[39] The interaction coefficients are incorporated in a dispersion energy expression, which is added as a correction to the base functional. In previous articles, it has been shown that XDM provides excellent accuracy in the calculation of molecular crystal lattice energies[18] (in the order of 1 kcal/mol) and that the energy differences are much better modeled because of error cancellation.[21]

Regarding the details of the periodic calculations, we used the Becke86b exchange[40] combined with the PBE correlation[41] functional in the Projector Augmented Wave (PAW) approach.[42] The relevant cutoff energies are 60 Ry for the plane wave cutoff and 600 Ry for the density cutoff. The k-point grid used is a 4 × 4 × 4 regular grid. The equivalent calculations on the monomers were carried out in cubic supercells 40 bohr in side with the same cutoffs but only one k-point at Γ. The geometries (cells and internal atomic positions) of all crystals and molecules were relaxed.

In order to evaluate the contributions of the different molecular contacts to the total lattice energy, we extracted selected dimers from the equilibrium crystal structures and calculated the binding energy in the gas phase, with the geometry of the monomers frozen in their crystal structures. These calculations neglect cooperative and crystal polarization effects but allow comparing contact based directional interactions. In addition, these calculations neglect monomer deformation energies (the energy necessary to deform the monomer from its gas phase structure to its geometry in the crystal structure), but this is useful in comparing interaction energies within the same crystal because the deformation energy is the same for all monomers.

The gas phase calculations were run using Gaussian09[43] and the LC-ωPBE functional[44,45] corrected with XDM dispersion.[38] To avoid excessive computational cost and improve the SCF convergence, we used the pc-2-spd basis set (that is, the pc-2 basis set[46−48] without the f primitives). We have shown in a recent article that this basis set is able to give noncovalent binding energy results close to the basis set limit at a greatly reduced computational cost.[49] As and Sb atoms are treated using the aug-cc-pVTZ basis set plus relativistic pseudopotentials.[50]

We used the noncovalent index (NCI) technique[24,25] to visualize the relevant intermolecular interactions in the crystal structures at the equilibrium geometries. NCI uses electron density descriptors to identify the relevant interacting contacts

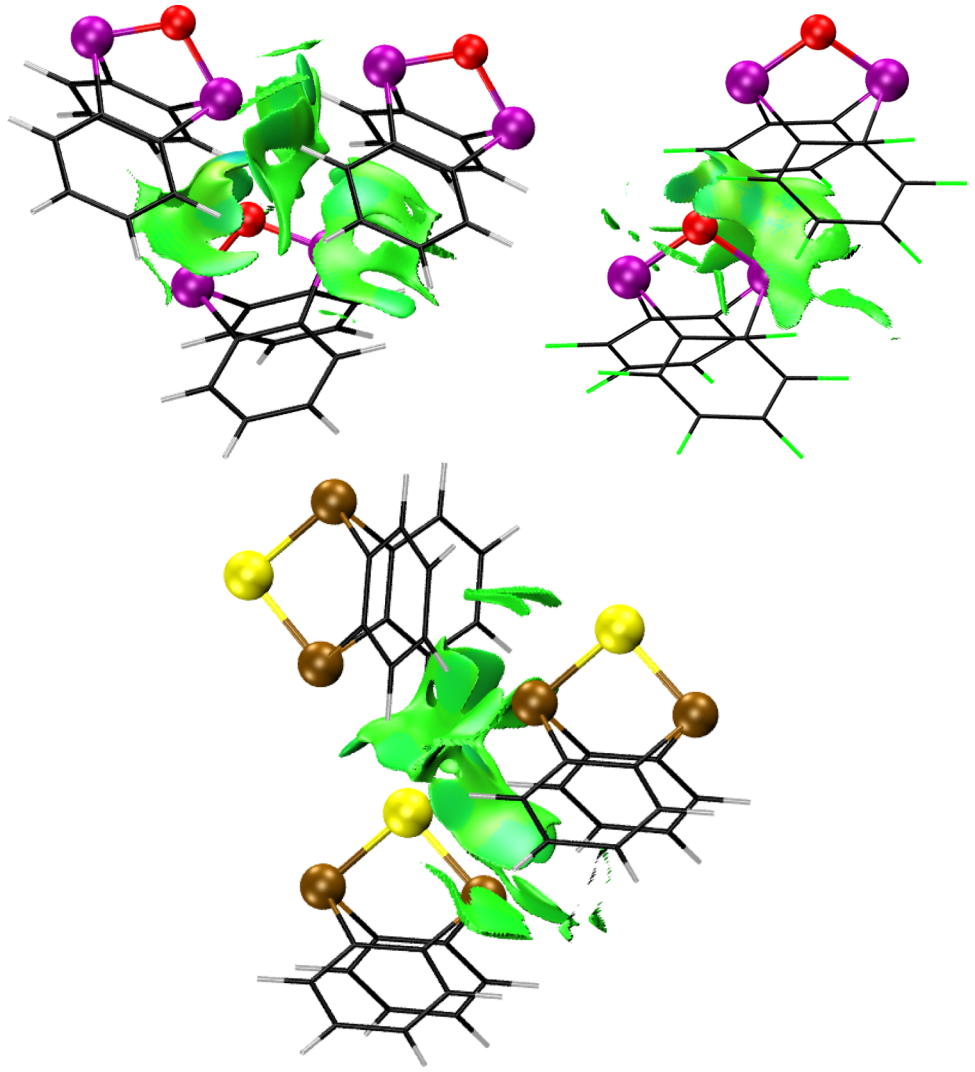

Figure 4. NCI plots for the EPXARS (top left), FEPXAS (top right), and EPSARS (bottom) crystals at the equilibrium geometry. Only a fraction of the crystal depicting the relevant motif is shown.

of two molecules and has been used before in the study of halogen bonds.[16] The NCI technique plots isosurfaces of the reduced density gradient:

$$s = \frac{1}{2(3\pi^2)^{1/3}} \frac{|\nabla\rho|}{\rho^{4/3}} \quad (1)$$

On the surfaces, a color mapping scheme is used based on the value of the electron density times the sign of the second eigenvalue of the Hessian. Strong intermolecular interactions corresponding to a high intermolecular electron density appear as a blue localized region, whereas extensive weak contacts appear as large green regions. Intermolecular densities have been related to binding energies in the particular case of pnictogen bonds.[11] We used the critic2 program[51,52] for the calculation of the NCI index from the calculated periodic densities.

In the crystal geometry discussion we followed the CSD criteria regarding van der Waals radii.[7] That is, the radii are taken from Bondi[53] (F, 1.47 Å; As, 1.85 Å; O 1.52 Å; S 1.80 Å; C 1.70 Å) except for hydrogen[54] (1.09 Å) and Sb, for which we take the arbitrary 2.0 Å value. We take the half thickness of a benzene ring as 1.8 Å.[8]

4. RESULTS

4.1. Intermolecular Contacts from NCI. Figure 4 shows the NCI plots for the EPXARS, FEPXAS, and EPSARS crystals at their equilibrium geometries. Three principal contacts can be identified in the 2D architecture of EPXARS: a double M···π (As···π) interaction, a M···X (As···O) interaction, and a M···M (As···As) interaction. The color intensity in these plots gives an idea of the interaction strength with the M···X contact being particularly relevant. The geometry of the three contacts is favorable for a donor−acceptor interaction, in which the lone pair donates charge to the σ-hole of the acceptor.[13,14] In the crystal, the molecules are oriented so that the donation occurs at the "back" of an intramolecular σ bond. In the case of the M···M bond, the geometry tells which M is the donor and which is the acceptor: the lone pair of one of the As is pointing to the σ-hole of the other As.

EPXARS is particularly interesting in that every As atom is involved in several contacts, acting as multiple donor or as donor and acceptor simultaneously. For every molecule in EPXARS (there is only one molecule in the asymmetric unit) one of the As atoms is an acceptor for three donors, corresponding to the back of every intramolecular σ bond it forms. The donors are the two π rings and the As atom of the

dx.doi.org/10.1021/ct500832g | J. Chem. Theory Comput. 2014, 10, 5010−5019

adjacent molecule, and they all form motifs that are aligned with the corresponding intramolecular σ bonds of the acceptor As. The other As acts as donor to the As of the adjacent molecule via its lone pair and as an acceptor from the chalcogen of the molecule below. Overall, each molecule in EPXARS is involved in eight donor/acceptor contacts, i.e., four As···π, two As···O, and two As···As. However, nothing in the crystal structure serves as an indication of the relative importance of these interactions, and the NCI plots only give a qualitative picture.

The FEPXAS crystal structure, which corresponds to the perfluorinated version of the EPXARS monomer, is substantially different from EPXARS. The primary effect of perfluorination on a benzene ring is to change its polarity and deplete the π cloud.[55] The quadrupole changes sign, and the behavior with respect to packing and donor−acceptor interactions is radically modified. In the case of FEPXAS the crystal is formed by stacked chains containing the interactions shown in Figure 4. The interaction is quite extensive, and we can identify As···O contacts as well as As···π contacts with the two π rings of the other molecule, although longer than in EPXARS. O···F contacts seem to happen as well, but the reduced extent of the NCI plot suggests that they are rather weak. The electrostatic dipole−dipole interaction between successive molecules, more favorably oriented than in EPXARS, is also a relevant packing feature and probably a contributing factor to the stability of this crystal.

EPSARS presents a 2D architecture similar to EPXARS but with a different arrangement of donor−acceptor contacts. In the case of EPSARS, the S and As atoms in different molecules form an almost orthogonal network of chalcogen-pnictogen bonds. Compared to EPXARS, the NCI plot domains show that the strength of the As···S interaction is comparatively weaker, but every sulfur atom engages in two donor−acceptor bonds instead of one. Given the strong directionality of these contacts, the orthogonal arrangement is the only allowed geometry that permits the double donor−acceptor interaction. The behavior of S compared to O follows the usual rules of donor−acceptor and covalent interactions: the S atom is larger so its ability to donate electrons is smaller, but it has more space around it to engage in more than one contact. There are also two additional contacts between As and π rings at different distances in EPSARS, shown in Figure 4.

4.2. Crystal Geometries. The relevant intramolecular geometry parameters for all crystals and the corresponding molecules in the gas phase are shown in Table 1. Selected intermolecular distances in the theoretical crystal structures are given in Table 2. The labels used in these tables correspond to those in Figures 1 and 3. The lattice energies and the binding energies of the relevant dimers at their crystal geometries will be discussed in detail in the next section; they are given in Table 3 and Table 4.

The defining feature[13,14] of donor−acceptor interactions is the donation from the electron rich donor to the σ-hole of the acceptor, located at the back of an intramolecular σ bond. Donor−acceptor interactions are strongly directional, and because an antibonding orbital in the acceptor is populated, the electron donation results in a weakening and lengthening of the acceptor intramolecular σ-bond located opposite to the intermolecular contact. The elongation of the intramolecular bond in the acceptor increases with the strength of the intermolecular interaction.

Table 1. Selected Intramolecular Angles and Distances for the Eight Molecules (M = As, Sb; X = O, S; and A = H, F) within the EPXARS, FEPXAS, and EPSARS Crystal Structures at Their Calculated Equilibrium Geometry[a]

phase	X	M	A	d_1	d_2	α	β
EPXARS	**O**	**As**	**H**	**1.871**	**1.902**	**113.0**	**108.1**
	O	As	F	1.845	1.932	113.3	109.8
	O	Sb	H	2.079	2.251	118.6	107.0
	O	Sb	F	2.037	2.241	115.6	110.0
	S	As	H	2.272	2.275	100.2	92.2
	S	As	F	2.259	2.266	103.8	93.3
	S	Sb	H	2.458	2.471	94.9	92.9
	S	Sb	F	2.445	2.450	103.2	94.3
FEPXAS	O	As	H	1.868	1.866	104.0	108.1
	O	**As**	**F**	**1.852**	**1.855**	**110.9**	**110.6**
	O	Sb	H	2.063	2.080	111.1	107.8
	O	Sb	F	2.055	2.090	119.7	110.7
	S	As	H	2.309	3.306	125.1	74.9
	S	As	F	2.259	2.270	110.5	93.3
	S	Sb	H	2.463	2.515	106.8	91.7
	S	Sb	F	2.444	2.476	112.5	94.2
EPSARS	O	As	H	1.869	1.874	98.0	108.2
	O	As	F	1.843	1.847	97.7	110.0
	O	Sb	H	2.095	2.070	113.0	107.5
	O	Sb	F	2.064	2.051	100.3	110.4
	S	**As**	**H**	**2.287**	**2.300**	**101.3**	**91.2**
	S	As	F	2.276	2.270	107.2	91.9
	S	Sb	H	2.516	2.503	101.3	91.4
	S	Sb	F	2.460	2.447	105.3	92.6
Vacuum	O	As	H	1.855	1.855	107.9	107.6
	O	As	F	1.847	1.847	107.0	110.0
	O	Sb	H	2.034	2.034	104.2	107.4
	O	Sb	F	2.027	2.027	103.6	110.3
	S	As	H	2.274	2.274	108.7	90.7
	S	As	F	2.268	2.268	107.5	92.6
	S	Sb	H	2.451	2.451	104.7	90.9
	S	Sb	F	2.447	2.449	104.0	93.4

[a]The geometries of the *in vacuo* molecules are also given ("Vacuum"). The labels correspond to Figure 1. Distances are in angstrom, and angles are in degrees. The values corresponding to the molecules that crystallize in the experimentally-observed EPXARS, FEPXAS, and EPSARS crystals are marked in bold.

This observation can be used to rationalize the intramolecular distances observed in the crystal packings (Table 1) and to obtain information about the attendant intermolecular donor−acceptor interactions. The intramolecular M−X distances (d_1 and d_2) are opposite to relevant intermolecular contacts in two of the phases studied: in EPXARS, the intramolecular distance d_1 corresponds to the bond opposite to the M···M intermolecular contact, and d_2 is opposite to the M···X contact. In EPSARS, the intramolecular bonds corresponding to d_1 and d_2 are aligned with intermolecular M···X contacts, forming an orthogonal two-dimensional framework. In FEPXAS, the same contacts do not correspond to a donor−acceptor interaction and are therefore closer to their gas phase values. This bond stretching effect is, in general, more significant in EPXARS for X=O than in EPXARS with X=S or in EPSARS, indicating a stronger donor−acceptor interaction in that particular case.

In EPXARS, the intermolecular contacts opposite to the d_1 and d_2 bonds are different, which introduces a certain degree of

Table 2. Selected Intermolecular Distances for the EPXARS, FEPXAS, and EPSARS Crystals at Their Equilibrium Structure Are Shown[a]

phase	X	M	A	d_{MX}	$d_M\pi$	d_{XA}	d_{MM}
EPXARS	O	As	H	**2.703**	**3.580**		**3.055**
	O	As	F	**2.471**	4.233		**3.092**
	O	Sb	H	**2.237**	**3.652**		**3.483**
	O	Sb	F	**2.241**	4.138		**3.507**
	S	As	H	**3.244**	3.660		**3.275**
	S	As	F	3.853	**3.592**		**3.290**
	S	Sb	H	**3.057**	**3.650**		**3.573**
	S	Sb	F	**3.631**	**3.616**		**3.590**
FEPXAS	O	As	H	3.500	3.715	2.738	
	O	As	F	**3.242**	**3.533**	**2.856**	
	O	Sb	H	**2.984**	**3.551**	2.792	
	O	Sb	F	**2.742**	**3.490**	**2.928**	
	S	As	H	**2.274**	4.220	**2.800**	
	S	As	F	3.659	4.266	**3.168**	
	S	Sb	H	**3.079**	3.957	**2.889**	
	S	Sb	F	**3.234**	4.080	**3.094**	
EPSARS	O	As	H	3.572/3.871	4.104/3.760		
	O	As	F	3.956/4.842	4.658/4.126		
	O	Sb	H	**2.946**/3.850	4.323/ **3.599**		
	O	Sb	F	**2.905**/5.247	5.512/ **3.328**		
	S	As	H	**3.408**/ **3.463**	4.049/4.039		
	S	As	F	4.212/4.312	3.996/4.817		
	S	Sb	H	**3.124**/ **3.311**	4.079/3.941		
	S	Sb	F	4.248/4.136	4.002/4.904		

[a]The labels correspond to Figure 3. The values marked in bold are lower than the sum of the corresponding van der Waals radii. Distances are in angstrom.

Table 3. Lattice Energies (in kcal/mol) for the Three Different Crystal Packings Are Shown (E_{latt})[a]

			EPXARS		FEPXAS		EPSARS	
X	M	A	E_{latt}	E_{latt}^{disp}	E_{latt}	E_{latt}^{disp}	E_{latt}	E_{latt}^{disp}
O	As	H	26.04	31.55	23.07	30.23	24.07	31.14
O	As	F	17.52	27.35	16.85	25.71	13.91	22.91
O	Sb	H	35.92	32.86	27.19	33.00	28.66	34.52
O	Sb	F	26.72	29.43	20.82	28.64	21.11	30.52
S	As	H	21.70	28.05	14.36	16.64	26.59	33.49
S	As	F	15.59	24.95	14.32	23.63	19.44	29.10
S	Sb	H	25.05	29.64	16.16	18.27	30.68	36.05
S	Sb	F	17.74	27.54	15.64	26.69	20.64	30.03

[a]The dispersion contribution (E_{latt}^{disp}), which is a component of the lattice energy, is also given.

asymmetry in the monomer not found in the other two crystals or in the gas phase. The d_2 distance, which corresponds to the bond opposite to the M···X intermolecular interaction, is systematically longer than the one opposite to the M···M interaction, indicating that the former is stronger than the latter. The donor−acceptor M···X contact in EPXARS with X=S is, in contrast, not very efficient; the intramolecular distances in the crystal are close to their values in the isolated molecule. All these observations correlate nicely with the frozen monomer binding energies listed in Table 4, indicating that certain descriptors based on the equilibrium structure alone, such as the intramolecular distances behind a donor−acceptor interaction, can be used as faithful indicators of interaction strength.

In some particular crystal packings, the asymmetry of the intramolecular d_1 and d_2 distances becomes extreme because of a significant distortion of the monomer structure. This is observed for EPXARS O−Sb−H and O−Sb−F and for FEPXAS S−As−H. In these three crystals, the intermolecular donor−acceptor interactions are so strong that they effectively become dative bonds. While these crystal packings are unlikely to be observed experimentally, they show that dative bonds are at the limit of very strong noncovalent donor−acceptor interactions. In EPXARS O−Sb−H and O−Sb−F, a triangular Sb_3O motif involving the Sb−O−Sb in a molecule and the Sb in its neighbor is formed, with three Sb−O distances of approximately the same length. As shown in Table 1, the monomer geometry in the crystal is only slightly deformed. The Sb_3O triangular motif is particularly favorable in terms of energy: the EPXARS O−Sb−H and O−Sb−F crystals are significantly more stable than their As counterparts and the most stable in this particular crystal phase. The formation of an intermolecular dative bond confirms the importance of the M··· X donor−acceptor interaction in EPXARS. If the acceptor is good enough, the interaction is so favorable that a very short bond is formed.

In FEPXAS S−As−H, one-dimensional chains of dative M− X bonds are formed along the c crystallographic direction. In contrast with Sb-containing EPXARS, this is one of the most unstable FEPXAS crystals (Table 3) but presents one of the most stable intermolecular interactions (Table 4). The reason for this is probably in the large energy required to deform the FEPXAS monomer from its gas phase structure to its structure in the crystal. This can be clearly seen in how the π angle (α) is overly widened compared to its vacuum value and how the triangular intramolecular M−X−M motif (the β angle) is severely deformed.

dx.doi.org/10.1021/ct500832g | J. Chem. Theory Comput. 2014, 10, 5010−5019

Table 4. Table of Binding Energies of the Dimers at Their Geometry in the Crystal Referred to the Frozen Monomers[a]

			EPXARS(MX)		EPXARS(Mπ)		EPXARS(MM)		FEPXAS	
X	M	A	BE	BE^{disp}	BE	BE^{disp}	BE	BE^{disp}	BE	BE^{disp}
O	As	H	12.65	8.80	8.73	10.51	4.56	5.51	11.45	10.00
O	As	F	14.70	10.62	7.03	8.09	1.79	2.79	14.01	12.96
O	Sb	H	26.85	10.85	9.62	12.21	5.49	6.33	20.07	14.24
O	Sb	F	27.69	12.09	7.75	9.64	2.70	3.81	22.74	16.81
S	As	H	4.92	6.08	11.01	10.68	2.91	4.12	23.86	9.99
S	As	F	3.27	4.25	11.15	12.37	1.93	2.47	6.73	7.95
S	Sb	H	5.88	7.05	14.48	11.82	3.36	4.90	12.70	11.75
S	Sb	F	4.50	5.54	13.57	13.96	2.37	3.31	8.50	11.19

			EPSARS(Xπ)		EPSARS(MX)		EPSARS(MX′)	
X	M	A	BE	BE^{disp}	BE	BE^{disp}	BE	BE^{disp}
O	As	H	3.97	6.80	10.33	9.59	4.39	2.93
O	As	F	3.59	4.38	6.76	8.18	1.47	1.30
O	Sb	H	4.60	7.28	19.62	14.01	4.79	3.58
O	Sb	F	1.47	3.14	22.05	16.86	4.24	3.62
S	As	H	5.52	7.67	9.11	9.29	4.64	3.72
S	As	F	10.48	11.56	7.00	7.12	1.98	1.85
S	Sb	H	6.91	8.67	12.58	11.65	6.50	4.97
S	Sb	F	12.26	12.90	7.48	7.69	2.60	2.32

[a]All energies in kcal/mol. Three dimers are given for EPXARS and EPSARS, which correspond to the three possible molecule pairs in Figure 3. The dimers are labeled according to the dominant interaction (in EPSARS, MX and MX′ are two different M···X contacts). Only one intermolecular contact is possible in FEPXAS. The dispersion contribution (labeled BE_{disp}) is also shown.

Table 2 shows the intermolecular distances in the crystals compared to the sum of van der Waals radii. Note that the van der Waals radii are averages over experimental structures and thus slightly large when compared to DFT results due to missing vibrational effects. In EPXARS, the d_{MX} distances corresponding to the M···X interaction are significantly shorter than the sum of van der Waals radii for X=O (As···O, 3.37 Å, Sb···O, 3.52 Å) indicating a strong interaction. For X=S, the interaction is weaker, with distances close to or above the sum of their van der Waals radii (As···S, 3.65 Å, Sb···S, 3.80 Å). This is consistent with the preceding discussion and confirmed by the binding energies in Table 4, where X=O has binding energies in the range 10−30 kcal/mol, whereas X=S is in the range 3−6 kcal/mol. The effect of fluorination in EPXARS is small and toward greater binding energies in X=O and toward weaker binding in X=S, as shown by both intermolecular distances and binding energies.

The intermolecular distances can also be compared between polymorphs of the same monomer. The As···X distance is shorter in EPXARS than in the equivalent FEPXAS crystal for X=O, whereas it is slightly longer for X=S. Thus, the As···O interaction is significantly stronger in EPXARS than in FEPXAS. The binding energies in Table 4 confirm that M···X is the leading contribution in EPXARS in the X=O case but only a minor stabilizer for X=S. Unfortunately, it is not possible to separate the M···X interaction from the rest in the binding energies of FEPXAS. Fluorination promotes the M···X interaction in EPXARS by improving the acceptor character of the M atom.

The intermolecular d_{MX} distances in EPSARS show two regimes. In the X=O crystals, the two d_{MX} distances are clearly asymmetric for M=Sb, indicating a single Sb···O interaction coupled with a relatively stronger M···π interaction. The same interaction is not possible in the M=As case, and the corresponding crystals are less stable, as revealed by the lattice energies in Table 3. The second bonding regime happens in the M=S crystals, where the two intermolecular distances are roughly equivalent and shorter than the van der Waals radii sum, indicating that every sulfur atom engages as donor in two M···X contacts, in the almost orthogonal arrangement shown in Figure 2. Such an arrangement, however, is prevented in the A=F versions of these crystals, probably because the larger size of the fluorinated phenyls prevents the close packing of the molecules. For instance, the calculated equilibrium cell volume of S−As−F EPSARS is 1298.2 $Å^3$, whereas that of S−As−H is only 1072.5 $Å^3$. The double M···X contact stabilizes the A=H crystals with respect to the A=F, as shown in Table 3.

The nature of the M···π interactions in the crystals can also be studied using the distances in Table 2. In EPXARS X=O, the M···π distance is well below the sum of van der Waals radii for A=H. The reverse occurs in FEPXAS: the M···π distance is shorter for A=F than for A=H. Also, the binding energies in Table 4 confirm that the interaction is stronger with hydrogenated than fluorinated benzene rings in EPXARS. These observations suggest that the nature of the M···π interaction is different in EPXARS from that in FEPXAS. In EPXARS, the behavior of the M···π contact under fluorination is what one would expect from a donor(π)−acceptor(M) interaction. In FEPXAS, the M···π interaction behaves as a lone pair(M)···π, in which fluorination increases binding by depleting the π-electron cloud. The crystal geometry is a clear indication as well: while in EPXARS, the π rings are oriented toward the σ holes of the M, the same does not happen in FEPXAS. Replacement of X by sulfur seems to weaken the M···π interaction in FEPXAS, perhaps caused by steric effects and the competition with the M···X interaction. The binding energies are also decreased.

In EPSARS, the M···π interaction is relatively weak except in the Sb−O crystals, where this contact appears as a substitute for the single intermolecular Sb···O bond. Lattice energies (Table 3) show an increased stabilization with respect to the equivalent As−O crystals, which could be explained by the increased

acceptor strength of Sb compared to As. Interestingly, the molecular arrangement in EPSARS shows a X···π (lone pair···π) interaction that is missing in the other two crystal packings. Table 4 shows that this interaction is favored for X=S relative to X=O and also by the perfluorination of the ring in X=S. This indicates that S acts as the donor and the π ring as the acceptor in the X=S crystals.

Lastly, the M···M distance in EPXARS is in all cases below the sum of van der Waals radii. However, Table 4, the intramolecular d_1 and d_2 distances, and the NCI plots show that this interaction is weaker than the M···X and M···π interactions in stabilizing the crystal structure. Substitution of X and A seem to have only a minor effect both in the distances and in the binding energies.

4.3. Lattice Energies. How does all the information in the preceding section come together to interpret the actual crystal packings? Table 3 lists the calculated lattice energies for the 24 considered crystal structures. The data show that EPXARS is in all cases more stable than FEPXAS with a difference in lattice energy that ranges from 8.9 kcal/mol (S−Sb−H) down to 0.7 kcal/mol in O−As−F, the latter corresponding to the experimentally observed FEPXAS crystal. This is no surprise given the greater number of donor−acceptor interactions in EPXARS. EPSARS has a stability similar to FEPXAS in the X=O crystals (the maximum difference between them is 2.9 kcal/mol in O−As−F). However, for X=S, EPSARS is notably more stable than EPXARS (2.9 to 5.6 kcal/mol), and particularly FEPXAS (5.0 to 14.5 kcal/mol), because of sulfur's ability to engage as a donor in multiple M···X interactions, as discussed in the preceding section.

EPXARS O−As−H and EPSARS S−As−H are more stable than the other phases by at least 2.0 and 4.9 kcal/mol, respectively, which is in agreement with experiment. In the O−As−F case, the lattice energy of EPXARS is also higher, but only 0.7 kcal/mol greater than FEPXAS, which is within the error bar for calculated lattice energies (∼1 kcal/mol).[37] The crystallization in the FEPXAS structure may also be affected by kinetic factors (e.g., solvent effects during nucleation and growth). Regardless of the phase or substituents, the presence of Sb always stabilizes the crystal compared to As, probably due to its improved acceptor character. Regrettably, experimental crystal structures are not available for comparison.

According to the lattice energies, all crystal polymorphs are more stable for A=H than for A=F. In EPXARS, fluorination increases the binding energy of the M···X interaction in X=O and of the M···π interaction in X=S. This indicates that the character of the interaction changes from donor−acceptor to lone pair···π upon substitution of O to S, in agreement with the previous discussion using the intermolecular distances. In EPSARS, fluorination enables the X···π interaction (as shown in Table 4), but it also destroys the double M···X interaction with M=S, resulting in a smaller lattice energy. Except in the case of EPSARS, oxygen leads to more stable crystals than sulfur. Specifically, O decreases the stability of the M···π contact, but this is more than accounted for by the increased stability of the M···X. However, the EPSARS geometry relies on the formation of multiple M···X contacts, which can be attained more easily by S than by O due to its larger size.

To summarize our results, EPXARS is stabilized by a combination of donor−acceptor M···π and M···X interactions and weaker M···M interactions. FEPXAS is stabilized by a M···X contact and by a lone pair···π interaction. Hydrogenated phenyl rings favor donor−acceptor M···π and M···M interactions and so EPXARS is more stable. However, upon fluorination, the donor−acceptor M···π and M···M interactions are weakened and the lone pair···π interaction is stabilized, and so EPXARS and FEPXAS acquire similar stability, which explains why FEPXAS is experimentally observed. Note, however, that the lattice energy of FEPXAS still decreases on fluorination despite all the relevant distances and the binding energy (Table 4) indicating a more stable interaction. We speculate that this is caused by less efficient chain packing in the A=F FEPXAS crystal than in A=H. The cell lengths perpendicular to the chain direction in A=F FEPXAS are a = 14.5 Å and b = 18.7 Å, while they are only a = 12.7 Å and b = 16.1 Å for A = H. Less efficient packing is apparent in the decreased dispersion contribution, that mirrors the drop in total lattice energy.

Regarding EPSARS, its crystal packing favors that the X atom engages in multiple M···X interactions, and, as a result, the M=S phases have greater stability than M=O, due to its ability to coordinate to more than one acceptor. The double M···X interaction is disrupted by perfluorination, in which case it is replaced by a lone pair (X)···π interaction, which is weaker in comparison.

Finally, we note that dispersion effects are relatively more important in the crystal phase than in the gas phase dimers. This is a reasonable result[6,56] because molecular crystals are closely packed, and it is expected that dispersion plays a more important role in the overall stabilization of the crystal structure than inferred from gas phase dimer binding energies. For instance, the sum of the three dimer interactions in EPXARS O−As−H (Table 4) gives a binding energy per molecule of 25.9 kcal/mol, comparable to the actual lattice energy (26.0 kcal/mol, Table 3). However, the sum of the dispersion contributions to the dimer binding energies gives only 24.8 kcal/mol, whereas in the crystal the dispersion contribution to the lattice energy is much higher (31.6 kcal/mol). These numbers, however, should be interpreted with care because the dispersion contribution in dcDFT accounts not only for the missing dispersion interactions but also for errors in the modeling of the nondispersive part of the noncovalent interaction coming from the base functional. The dispersion contribution exceeds the lattice energy in all our crystals (Table 3) indicating that they also play a major role in determining the crystal geometries.

5. CONCLUSIONS

In this article, we have presented a method for the analysis of intermolecular interactions in crystal packings. The procedure is analogous to model dimer gas phase studies in that it involves molecular analogues where some of the atoms have been substitued in order to tune the electronic properties of the monomer. However, the substitution takes place in the actual crystal structure, and we use density functional theory with the exchange hole dipole moment (XDM) dispersion correction to find the equilibrium geometries and relative stabilities of the crystals. The resulting crystal structures are combined with the noncovalent interaction (NCI) index, with frozen monomer gas phase binding energy calculations at the crystal geometry and with the analysis of the crystal geometries. We show how this procedure is useful in extracting information about the leading contributions determining the stability of a particular crystal packing.

In order to illustrate the technique, we have calculated the structures of the crystals composed of derivatives of 5,10-epoxy-

5,10-dihydroarsanthrene, $As_2(C_6H_4)_2O$. The monomers, shown in Figure 1, contain two pnictogens (which we label M), a chalcogen (X), and two π rings. As a result, a multitude of donor−acceptor interactions are present in the crystal packing, sometimes involving the same atom. Three experimental crystals that these molecules present have been studied (Figure 2): the structure of the $As_2(C_6H_4)_2O$ crystal itself (called EPXARS), the phase of the same perfluorinated monomer (FEPXAS), and the $As_2(C_6H_4)_2S$ crystal (EPSARS). In EPXARS, a two-dimensional architecture is formed involving pnictogen-pnictogen, pnictogen-chalcogen, and pnictogen-π interactions. FEPXAS contains one-dimensional chains of aligned dipoles with a clear As···O interaction and a weaker As···π interaction. EPSARS shows an orthogonal arrangement of As···S chains where each sulfur acts as donor to two As atoms. The motifs are shown in Figure 3.

Using our procedure, we show that an important contribution in the three crystals is the M···X (As···O/S) contact together with M···π and X···π interactions. The M···π and X···π interactions have different characters in different crystals or even in analogues of the same crystal. In EPXARS, M···π behaves as a donor(π)−acceptor(As), whereas in FEPXAS it is a lone pair(As)···π. In EPSARS, X···π behaves as a lone pair···π as well. The M···M interaction is only present in EPXARS and is in all cases weaker than M···X. EPXARS is more stable than FEPXAS in general except in the case where As−O−F is perfluorinated, where the M···M and M···π interactions in EPXARS decrease in importance, the lone pair···π interaction is stabilized, and EPXARS and FEPXAS have roughly the same lattice energy. EPSARS is the more stable crystal in the M=S case due to the ability of sulfur to act as donor to two acceptor atoms. The lattice energies (except in FEPXAS) are in agreement with the crystal structures observed in experiment. Packing effects, dominated by dispersion interactions, are important, with perfluorination leading in general to a less compact crystal structure and a decrease in the stabilizing contribution coming from dispersion.

AUTHOR INFORMATION

Corresponding Authors

*E-mail: alberto.oterodelaroza@nrc-cnrc.gc.ca.
*E-mail: victor@fluor.quimica.uniovi.es.
*E-mail: edward.tiekink@gmail.com.
*E-mail: julio@power.ufscar.br.

Notes

The authors declare no competing financial interest.

ACKNOWLEDGMENTS

A.O.R. and V.L.C. thank the Spanish Malta/Consolider initiative (no. CSD2007-00045). V.L.C. thanks the Spanish MINECO, project number CTQ2012-31174. This work is supported by the High Impact Research MoE Grants UM.C/625/1/HIR/MoE/SC/-03 and -12 from the Ministry of Higher Education, Malaysia. J.Z.-S. thanks the Brazilian agency CNPq for a fellowship (305626/20132).

REFERENCES

(1) Desiraju, G. R. *Angew. Chem., Int. Ed.* **1995**, *34*, 2311−2327.
(2) Desiraju, G. R. *Chem. Commun.* **1997**, 1475−1482.
(3) Johnson, D. W.; Lindquist, N. R.; Carnes, M. E. *Encyclopedia of Supramolecular Chemistry*; Chapter 122, pp 1−17.
(4) Desiraju, G. R. *J. Am. Chem. Soc.* **2013**, *135*, 9952−9967.
(5) Tiekink, E. R. T. *Chem. Commun.* **2014**, *50*, 11079−11082.
(6) Taylor, R. *CrystEngComm* **2014**, *16*, 6852−6865.
(7) Allen, F. H. *Acta Crystallogr., Sect. B: Struct. Sci.* **2002**, *58*, 380−388.
(8) Zukerman-Schpector, J.; Otero-de-la-Roza, A.; Luaña, V.; Tiekink, E. R. T. *Chem. Commun.* **2011**, *47*, 7608−7610.
(9) Mooibroek, T. J.; Gamez, P.; Reedijk, J. *CrystEngComm* **2008**, *10*, 1501−1515.
(10) Jain, A.; Purohit, C. S.; Verma, S.; Sankararamakrishnan, R. *J. Phys. Chem. B* **2007**, *111*, 8680−8683.
(11) Bauzá, A.; Quiñonero, D.; Deyà, P. M.; Frontera, A. *Phys. Chem. Chem. Phys.* **2012**, *14*, 14061−14066.
(12) Otero-de-la-Roza, A.; Mallory, J. D.; Johnson, E. R. *J. Chem. Phys.* **2014**, *140*, 18A504.
(13) Scheiner, S. *Acc. Chem. Res.* **2012**, *46*, 280−288.
(14) Scheiner, S. *Int. J. Quantum Chem.* **2013**, *113*, 1609−1620.
(15) Hunter, C. A.; Sanders, J. K. M. *J. Am. Chem. Soc.* **1990**, *112*, 5525−5534.
(16) Kozuch, S.; Martin, J. M. L. *J. Chem. Theory Comput.* **2013**, *9*, 1918.
(17) Moilanen, J.; Ganesamoorthy, C.; Balakrishna, M. S.; Tuononen, H. M. *Inorg. Chem.* **2009**, *48*, 6740−6747.
(18) Otero-de-la-Roza, A.; Johnson, E. R. *J. Chem. Phys.* **2012**, *137*, 054103.
(19) Johnson, E. R.; Mackie, I. D.; DiLabio, G. A. *J. Phys. Org. Chem.* **2009**, *22*, 1127.
(20) DiLabio, G. A.; Otero-de-la-Roza, A. In *Rev. Comput. Chem.*; Lipkowitz, K. B., Ed.; Wiley-VCH: Hoboken, NJ, 2014; (in press), arXiv: 1405.1771.
(21) Otero-de-la-Roza, A.; Cao, B. H.; Price, I. K.; Hein, J. E.; Johnson, E. R. *Angew. Chem., Int. Ed.* **2014**, *126*, 8013−8016.
(22) Day, G. M.; Cooper, T. G.; Cruz-Cabeza, A. J.; Hejczyk, K. E.; Ammon, H. L.; Boerrigter, S. X. M.; Tan, J. S.; Della Valle, R. G.; Venuti, E.; Jose, J.; Gadre, S. R.; Desiraju, G. R.; Thakur, T. S.; van Eijck, B. P.; Facelli, J. C.; Bazterra, V. E.; Ferraro, M. B.; Hofmann, D. W. M.; Neumann, M. A.; Leusen, F. J. J.; Kendrick, J.; Price, S. L.; Misquitta, A. J.; Karamertzanis, P. G.; Welch, G. W. A.; Scheraga, H. A.; Arnautova, Y. A.; Schmidt, M. U.; van de Streek, J.; Wolf, A. K.; Schweizer, B. *Acta Crystallogr., Sect. B: Struct. Sci.* **2009**, *65*, 107−125.
(23) Bardwell, D. A.; Adjiman, C. S.; Arnautova, Y. A.; Bartashevich, E.; Boerrigter, S. X. M.; Braun, D. E.; Cruz-Cabeza, A. J.; Day, G. M.; Della Valle, R. G.; Desiraju, G. R.; van Eijck, B. P.; Facelli, J. C.; Ferraro, M. B.; Grillo, D.; Habgood, M.; Hofmann, D. W. M.; Hofmann, F.; Jose, K. V. J.; Karamertzanis, P. G.; Kazantsev, A. V.; Kendrick, J.; Kuleshova, L. N.; Leusen, F. J. J.; Maleev, A. V.; Misquitta, A. J.; Mohamed, S.; Needs, R. J.; Neumann, M. A.; Nikylov, D.; Orendt, A. M.; Pal, R.; Pantelides, C. C.; Pickard, C. J.; Price, L. S.; Price, S. L.; Scheraga, H. A.; van de Streek, J.; Thakur, T. S.; Tiwari, S.; Venuti, E.; Zhitkov, I. K. *Acta Crystallogr., Sect. B: Struct. Sci.* **2011**, *67*, 535−551.
(24) Johnson, E.; Keinan, S.; Mori-Sánchez, P.; Contreras-García, J.; Cohen, A.; Yang, W. *J. Am. Chem. Soc.* **2010**, *132*, 6498−6506.
(25) Otero-de-la-Roza, A.; Johnson, E. R.; Contreras-García, J. *Phys. Chem. Chem. Phys.* **2012**, *14*, 12165−12172.
(26) Kennard, O.; Wampler, D. L.; Coppola, J. C.; Motherwell, W. D. S.; Mann, F. G.; Watson, D. G.; MacGillavry, C. H.; Stam, C. H.; Benci, P. *J. Chem. Soc. C* **1971**, 1511−1515.
(27) Brown, D.; Massey, A.; Mistry, T. *J. Fluorine Chem.* **1980**, *16*, 483−487.
(28) Allen, D. W.; Coppola, J. C.; Kennard, O.; Mann, F. G.; Motherwell, W. D. S.; Watson, D. G. *J. Chem. Soc. C* **1970**, 810.
(29) Bauzá, A.; Alkorta, I.; Frontera, A.; Elguero, J. *J. Chem. Theory Comput.* **2013**, *9*, 5201−5210.
(30) Guan, L.; Mo, Y. *J. Phys. Chem. A* **2014**, *118*, 8911−8921.
(31) Steinmann, S. N.; Piemontesi, C.; Delacht, A.; Corminboeuf, C. *J. Chem. Theory Comput.* **2012**, *8*, 1629−1640.
(32) Giannozzi, P.; Baroni, S.; Bonini, N.; Calandra, M.; Car, R.; Cavazzoni, C.; Ceresoli, D.; Chiarotti, G. L.; Cococcioni, M.; Dabo, I.; Dal Corso, A.; de Gironcoli, S.; Fabris, S.; Fratesi, G.; Gebauer, R.; Gerstmann, U.; Gougoussis, C.; Kokalj, A.; Lazzeri, M.; Martin-Samos,

L.; Marzari, N.; Mauri, F.; Mazzarello, R.; Paolini, S.; Pasquarello, A.; Paulatto, L.; Sbraccia, C.; Scandolo, S.; Sclauzero, G.; Seitsonen, A. P.; Smogunov, A.; Umari, P.; Wentzcovitch, R. M. *J. Phys.: Condens. Matter* **2009**, *21*, 395502.
(33) Becke, A. D.; Johnson, E. R. *J. Chem. Phys.* **2005**, *122*, 154104.
(34) Becke, A. D.; Johnson, E. R. *J. Chem. Phys.* **2005**, *123*, 154101.
(35) Johnson, E. R.; Becke, A. D. *J. Chem. Phys.* **2006**, *124*, 174104.
(36) Becke, A. D.; Johnson, E. R. *J. Chem. Phys.* **2007**, *127*, 154108.
(37) Otero-de-la-Roza, A.; Johnson, E. R. *J. Chem. Phys.* **2012**, *136*, 174109.
(38) Otero-de-la-Roza, A.; Johnson, E. R. *J. Chem. Phys.* **2013**, *138*, 204109.
(39) Otero-de-la-Roza, A.; Johnson, E. R. *J. Chem. Phys.* **2013**, *138*, 054103.
(40) Becke, A. *J. Chem. Phys.* **1986**, *85*, 7184.
(41) Perdew, J.; Burke, K.; Ernzerhof, M. *Phys. Rev. Lett.* **1996**, *77*, 3865−3868.
(42) Blöchl, P. *Phys. Rev. B* **1994**, *50*, 17953.
(43) Frisch, M. J.; Trucks, G. W.; Schlegel, H. B.; Scuseria, G. E.; Robb, M. A.; Cheeseman, J. R.; Scalmani, G.; Barone, V.; Mennucci, B.; Petersson, G. A.; Nakatsuji, H.; Caricato, M.; Li, X.; Hratchian, H. P.; Izmaylov, A. F.; Bloino, J.; Zheng, G.; Sonnenberg, J. L.; Hada, M.; Ehara, M.; Toyota, K.; Fukuda, R.; Hasegawa, J.; Ishida, M.; Nakajima, T.; Honda, Y.; Kitao, O.; Nakai, H.; Vreven, T.; Montgomery, J. A., Jr.; Peralta, J. E.; Ogliaro, F.; Bearpark, M.; Heyd, J. J.; Brothers, E.; Kudin, K. N.; Staroverov, V. N.; Kobayashi, R.; Normand, J.; Raghavachari, K.; Rendell, A.; Burant, J. C.; Iyengar, S. S.; Tomasi, J.; Cossi, M.; Rega, N.; Millam, J. M.; Klene, M.; Knox, J. E.; Cross, J. B.; Bakken, V.; Adamo, C.; Jaramillo, J.; Gomperts, R.; Stratmann, R. E.; Yazyev, O.; Austin, A. J.; Cammi, R.; Pomelli, C.; Ochterski, J. W.; Martin, R. L.; Morokuma, K.; Zakrzewski, V. G.; Voth, G. A.; Salvador, P.; Dannenberg, J. J.; Dapprich, S.; Daniels, A. D.; Farkas, Ö.; Foresman, J. B.; Ortiz, J. V.; Cioslowski, J.; Fox, D. J. *Gaussian 09 Revision A.1*; Gaussian Inc.: Wallingford, CT, 2009.
(44) Vydrov, O. A.; Scuseria, G. E. *J. Chem. Phys.* **2006**, *125*, 234109.
(45) Vydrov, O. A.; Heyd, J.; Krukau, A. V.; Scuseria, G. E. *J. Chem. Phys.* **2006**, *125*, 074106.
(46) Jensen, F. *J. Chem. Phys.* **2001**, *115*, 9113−9125.
(47) Jensen, F. *J. Chem. Phys.* **2002**, *116*, 7372−7379.
(48) Jensen, F.; Helgaker, T. *J. Chem. Phys.* **2004**, *121*, 3463−3470.
(49) Johnson, E. R.; Otero-de-la-Roza, A.; Dale, S. G.; DiLabio, G. A. *J. Chem. Phys.* **2013**, *139*, 214109.
(50) Metz, B.; Stoll, H.; Dolg, M. *J. Chem. Phys.* **2000**, *113*, 2563−2569.
(51) Otero-de-la-Roza, A.; Blanco, M. A.; Martín Pendás, A.; Luaña, V. *Comput. Phys. Commun.* **2009**, *180*, 157−166.
(52) Otero-de-la-Roza, A.; Johnson, E. R.; Luaña, V. *Comput. Phys. Commun.* **2014**, *185*, 1007−1018.
(53) Bondi, A. *J. Phys. Chem.* **1964**, *68*, 441−451.
(54) Rowland, R. S.; Taylor, R. *J. Phys. Chem.* **1996**, *100*, 7384−7391.
(55) Reichenbächer, K.; Süss, H. I.; Hulliger, J. *Chem. Soc. Rev.* **2005**, *34*, 22−30.
(56) Kitaigorodskii, A. I. *Molecular crystals and molecules*; Academic Press: New York, 1973; pp 1−15.